Published in final edited form as:

Mol Cancer Ther. 2008 December ; 7(12): 3825–3833. doi:10.1158/1535-7163.MCT-08-0730.

1,1-Bis(3′-indolyl)-1-(*p*-chlorophenyl)methane activates the orphan nuclear receptor Nurr1 and inhibits bladder cancer growth

Teruo Inamoto[1], **Sabitha Papineni**[3], **Sudhakar Chintharlapalli**[3], **Sung-Dae Cho**[3], **Stephen Safe**[3], and **Ashish M. Kamat**[1,2]

[1]Department of Urology, The University of Texas M. D. Anderson Cancer Center, Houston, Texas

[2]Department of Cancer Biology, The University of Texas M. D. Anderson Cancer Center, Houston, Texas

[3]Institute of Biosciences and Technology, Texas A&M University Health Science Center, College Station, Texas

Abstract

Nurr1 is an orphan nuclear receptor and a member of the nerve growth factor I-B subfamily of transcription factors with no known endogenous ligand or stimulator. We show, for the first time, evidence that Nurr1 is expressed in a panel of 11 human bladder cancer cell lines. A new class of methylene-substituted diindolylmethanes (C-DIM) were screened and 1,1-bis(3′-indolyl)-1-(*p*-chlorophenyl)-methane (DIM-C-pPhCl) activated the ligand-binding domain of Nurr1. Treatment of bladder cancer cells with Nurr1-active C-DIM resulted in decreased cell survival (MTT assay) and induction of cell death pathways, resulting in poly(ADP-ribose) polymerase cleavage and DNA fragmentation. The specificity of the Nurr1-active compound was shown using RNA interference in 253J B-V cells, whereby small interfering RNA against Nurr1 attenuated ligand-dependent activation of Nurr1 and poly(ADP-ribose) polymerase cleavage. Furthermore, activation of Nurr1 resulted in stimulation of tumor necrosis factor-related apoptosis-inducing ligand and small interfering RNA experiments attenuated tumor necrosis factor-related apoptosis-inducing ligand production. In an orthotopic model of human bladder tumors established in nude mice, administration of a Nurr1-active C-DIM suppressed bladder cancer growth. These results identify Nurr1 as a potential target for bladder cancer therapy and also identify a novel agent for activating Nurr1.

Introduction

Urothelial carcinoma of the bladder is a common malignancy with an incidence of over 67,000 new cases per annum in the United States. Approximately 17,120 deaths resulted

Requests for reprints: Ashish M. Kamat, Departments of Urology and Cancer Biology, The University of Texas M. D. Anderson Cancer Center, Unit 1373, 1515 Holcombe Boulevard, Houston, TX 77030. Phone: 713-792-3250; Fax: 713-794-4824. akamat@mdanderson.org.

Disclosure of Potential Conflicts of Interest

A.M. Kamat: grant support from Bioniche, Abbott Molecular, Bayer, Tetralogic Pharmaceuticals, Halozyne, and Indevus; consultant to Plantacor. No other potential conflicts of interest were disclosed.

from urothelial carcinoma of the bladder in the United States in 2007, making this a significant health burden (1). Chemotherapy is the primary treatment modality for advanced urothelial carcinoma of the bladder, but median survival is only 12 to 14 months (2). Unfortunately, patients with progressive disease after initial chemotherapy have limited treatment options, and no therapy is known to prolong survival (3). It is thus extremely important that novel therapeutic agents be developed for treating urothelial carcinoma bladder.

Nuclear hormone receptors (NR) are ligand-activated transcription factors that regulate gene expression and are involved in reproduction, development, and general cellular function (4). All NR members display a highly conserved structural organization with a NH_2-terminal region (which encodes activation function-1) followed by the DNA-binding domain, a linker region, and the COOH-terminal region. The COOH-terminal region encodes the ligand-binding domain and a transcriptional domain, denoted as activation function-2 (4). A decade ago, gene products, which appeared to belong to the NR superfamily, were indentified based on their nucleic acid sequence identity. The endogenous signaling molecules or cognate ligands for these NRs are unknown; thus, the term “orphan receptor” was coined (5). Nur77 (NGIF-B/NR4A1), Nurr1 (NOT/NR4A2), and NOR-1 (MINOR/NR4A3) form a family of orphan NRs, with a highly conserved DNA-binding domain (91–95%) and COOH-terminal ligand-binding domain (60%) but minimal homology in their NH_2-terminal region (6). This subgroup of proteins functions as immediate-early response genes, which are induced by a wide range of physiologic signals, including growth factors, apoptosis inducers, inflammatory signals, and hormones, in a cell type-specific manner (5–7). Until recently, most studies have focused on expression patterns of NR4A family members in the brain where these receptors have been strongly implicated in Parkinson’s disease (8), schizophrenia (9), manic depression (10), and Alzheimer’s disease (11). However, recently this family of nuclear receptors have also being implicated in other vital cellular processes (7).

Nurr1 is an atypical member of the NR superfamily, which are primarily ligand-activated receptors, such as the glucocorticoid, estrogen, and retinoic acid receptors, which regulate gene expression via recognition of specific DNA-binding sequences (12). Nurr1 is important for dopaminergic neuron function via regulation of tyrosine hydoxylase expression (13). Preliminary reports suggest a role for Nurr1 in rheumatoid arthritis and cancer through modulation of apoptosis (14). Herein, we show that Nurr1 is expressed in bladder cancer cells and that it can affect cell growth, cell death, and tumor necrosis factor-related apoptosis-inducing ligand (TRAIL) production. We have indentified, for the first time, 1,1-bis(3′-indolyl)-1-(*p*-chlorophenyl)methane (DIM-C-pPhCl) as a novel Nurr1 transactivator. Moreover, DIM-C-pPhCl modulates Nurr1-dependent specific transcriptional activity, and DIM-C-pPhCl induces several apoptosis-related proteins. Our results suggest that Nurr1-active DIM-C-pPhCl is a potential novel agent for clinical treatment of bladder cancer.

Materials and Methods

Cell Culture and Diindolylmethanes

The cell lines used represent a wide range of human bladder cancer cell grades and stages. The UM-UC series of urothelial carcinoma lines (UM-UC3, UM-UC5, UM-UC6, UM-UC9, UM-UC10, UM-UC13, and UM-UC14 cells) were provided courtesy of H. Barton Grossman (The University of Texas M. D. Anderson Cancer Center). KU7 cells were supplied by William Benedict (The University of Texas M. D. Anderson Cancer Center). The 253J B-V cells were established as a highly tumorigenic variant from the 253J parental line through recycling in the mouse bladder as described previously (15). The methylene-substituted diindolylmethane (C-DIM) compounds were synthesized by condensation of substituted benzaldehydes (1 equivalent) and indoles (2 equivalents) essentially as described (16). The cell lines were maintained at 37°C in modified Eagle's MEM supplemented with 10% fetal bovine serum, vitamins, sodium pyruvate, L-glutamine, penicillin, streptomycin, and nonessential amino acids. All cells were plated at a density of 1.0×10^5/mL in medium supplemented with 10% fetal bovine serum, allowed to attach for 24 h, and then treated with either DIM-C-pPhCl or DMSO. DIM-C-pPhCl was dissolved in DMSO to yield a stock of 10 mmol/L, which was diluted into the culture medium to the indicated concentrations. In all experiments, cells were treated in log-phase growth.

ReverseTranscription-PCR

cDNAs were generated from 1 μg total RNAs from bladder cancer cells with or without 5 μmol/L DIM-C-pPhCl. Reverse transcription reaction was carried out using 1 μg RNA, 1 μmol/L Poly N primer (Operon Biotechnologies), 100 μmol/L deoxynucleotide triphosphates, and 0.25 units/μL reverse primer. PCR was carried out using 2 μg reverse transcription product as template with 200 μmol/L deoxynucleotide triphosphates, 0.65 unit Amplitaq polymerase, 10× buffer, 500 nmol/L forward primer, and 500 nmol/L reverse primer. PCR was done as follows: a 5 min denaturation at 96°C, 25 cycles of 30 s at 94°C, 1 min annealing at 60°C, and 1 min extension at 72°C followed by a final extension for 5 min at 72°C. The primer sequences for the genes of interest were as follows: human TRAIL 5′-TTCACAGTGCTCCTGCAGTC-3′ (sense) and 5′-CAGCAGGGGCTGTTCATACT and human glyceraldehyde 3-phosphate dehydrogenase 5′-GAGTCAACGGATTTGGTCGT-3′ (sense) and 5′-TTGATTTTGGAGGGATCTCG-3′ (antisense).

Transfection and Luciferase Assay

KU7 cells were plated in 24-well plates at 1×10^5 in DMEM/Ham's F-12 supplemented with 2.5% charcoal-stripped fetal bovine serum. GAL4-Nurr1 chimera and the GAL4-Nur77 was provided by Dr. Jae W. Lee (Baylor College of Medicine). The GAL4 reporter containing five GAL4 response elements (pGAL4) was provided by Dr. Marty Mayo (University of North Carolina). After growth for 24 h, various amounts of DNA [GAL4Luc (0.4 μg), β-galactosidase (0.04 μg), and GAL4-Nurr1 (0.04 μg)] were transfected by LipofectAMINE plus reagent (Invitrogen) according to the manufacturer's protocol. After 5 to 6 h of transfection, cells were treated with complete medium containing either vehicle (DMSO) or the indicated ligands for 20 to 22 h. Cells were then lysed with 100 μL of 1× reported lysis buffer (Promega), and 30 μL cell extract was used for luciferase and β-galactosidase assays.

Lumicount was used to quantitate luciferase and β-galactosidase activities, and the luciferase activities were normalized to β-galactosidase activity.

Reagents and Antibodies

Rabbit antibodies to Nurr1 and TRAIL were purchased from Santa Cruz Biotechnology. Rabbit antibody to Nur77 was purchased from IMGENEX. Mouse antibodies to cleaved poly(ADP-ribose) polymerase (PARP) and cas-pase-3 and rabbit antibodies to caspase-8 and caspase-9 were obtained from Cell Signaling Technology.

Quantification of Apoptosis

Apoptosis was measured by propidium iodide staining and fluorescence-activated cell sorting analysis as described previously (19). Harvested cancer cells were pelleted by centrifugation and resuspended in a PBS containing 50 μg/mL propidium iodide, 0.1% Triton X-100, and 0.1% sodium citrate. Samples were stored at 4°C for 16 h and gently vortexed before fluorescence-activated cell sorting analysis.

Small Interfering RNA-Mediated Silencing of Endogenous Nurr1

To silence endogenous Nurr1, small interfering RNA (siRNA) oligo-targeting Nurr1 was purchased from Ambion: sense 5′-GGCUUGUAAAUUUACCCAATT-3′ and antisense 5′-UUGGGUAAAUUUACAAGCCTT-3′. As nontargeting control, Silencer Negative Control siRNA (Ambion) was used. Cells were grown to 60% confluency in six-well plates and transfected with specific or nonspecific siRNA using Oligofectamine reagent (Invitrogen/Life Technologies) according to the manufacturer's protocols.

Orthotopic Tumor Model Using Bioluminescent Imaging

Animal maintenance and experiments were done according to institutional guidelines established by the Animal Core Facility at The University of Texas M. D. Anderson Cancer Center. *In vivo* xenograft growth was evaluated in 6-week-old male athymic mice (purchased from the NIH). Bioluminescent imaging was done on all mice weekly using the IVIS imaging system as described previously (17). In brief, cultured 253J B-V cells with a stably transfected luciferase gene grown to 70% confluence were harvested with 0.1% EDTA/0.25% tryspin, washed, and resuspended in HBSS (Invitrogen) for injection. Mice were anesthetized by i.p. injection of pentobarbital. After exposure of the bladder through a lower abdominal incision, 2×10^5 tumor cells in 100 μL were injected into the muscle wall of the bladder dome. One week after tumor inoculation, mice were divided into three groups to yield even distribution of tumor sizes by luminescence. Starting that same day, group 1 received i.p. injection of 100 μL DMSO three times a week, and groups 2 and 3 received 25 and 50 mg/kg C-DIM reconstituted in 100 μL DMSO three times a week, respectively. Bioluminescent imaging was done on all mice weekly using the IVIS imaging system 10 min after i.p. injection of 3 mg firefly luciferin. Tumorigenicity was also assessed by necropsy after 4 weeks of therapy.

Immunohistochemistry

Formalin-fixed, paraffin-embedded tumor sections (4–5 μm) were deparaffinized in xylene and rehydrated using graded ethanols. After deparaffinization, antigen retrieval was done by heating the sections in a microwave oven in 10 mmol/L Tris/1 mmol/L EDTA (pH 9.0) buffer followed by washes with water. A mouse anti-proliferating cell nuclear antigen (PCNA) antibody (DAKO) was used for PCNA immunostaining. After incubation with rat anti-mouse IgG2a horseradish peroxidase (Serotec/Harlan Bioproducts) for 1 h at room temperature, stable DAB (Research Genetics) was used for visualization of the antigen-antibody complex. Sections were lightly counter-stained with hematoxylin. Some tissue samples were concomitantly stained with H&E. The intensity of the immunostaining was quantified in multiple points in five different areas of each sample by an image analyzer using MetaMorph (Universal Imaging) to obtain an average measurement. The density of proliferative cells and apoptotic cells was expressed as an average of the five highest densities identified within a single ×200 field.

In situ Labeling of Fragmented DNA (Terminal Deoxynucleotidyl Transferase-Mediated dUTP Nick End Labeling Staining)

Slide-mounted tissue sections were brought to room temperature and were deparaffinized. Subsequently sections were covered with 50 μL labeling solution containing biotin-16-dUTP (Roche Diagnostics) diluted 1:200 and terminal transferase (Invitrogen) and incubated for 60 min at 37°C. After incubation with 1:300 horseradish peroxidase-conjugated streptavidin for 1 h at room temperature, labeled nuclei were visualized using the Stable DAB (Research Genetics). Sections were lightly counterstained with hematoxylin. Terminal deoxynucleotidyl transferase-mediated dUTP nick end labeling (TUNEL) index was decided using commercial kit (Promega) according to the instructions of the manufacturer with small modification. In brief, frozen tissue sections fixed and treated in the preceding section were washed with PBS containing 0.1% Brij. Subsequently, sections were covered with 50 μL labeling solution containing fluorescein-dUTP diluted 1:200 and terminal transferase (Invitrogen) and incubated for 60 min at 37°C protected from light. After washing them to remove unincorporated fluorescein-dUTP, background reactivity was determined by processing the slides in the absence of terminal deoxynucleotidyl transferase (negative control). Nuclei were stained with propidium iodide (1 μg/mL) for 10 min. Immunofluorescence microscopy was done using a Zeiss Plan-Neofluar lens on an epifluorescence microscope equipped with narrow band-pass excitation filters mounted in a filter wheel (Ludl Electronic Products) to individually select for green, red, and blue fluorescence. Images were captured using a cooled charge-coupled device camera (Photometrics). DNA fragmentation was detected by localized green fluorescence within the nucleus of apoptotic cells.

SDS-PAGE and Immunoblotting

SDS-PAGE and immunoblotting was done as described previously (18). Cells were for 30 min on ice in radioimmunoprecipitation assay buffer containing protease and phosphatase inhibitors. Subsequently, extracted proteins were separated on either 10% or 12% SDS-PAGE gel, and the fractionated proteins were transferred to a polyvinylidene difluoride

membrane (Immobilon-P; Millipore). Specific antigens were probed by the corresponding monoclonal antibodies followed by horseradish peroxidase-conjugated secondary antibody (Invitrogen). Western blots were visualized by the enhanced chemiluminescence technique (Perkin-Elmer Life Sciences).

Statistical Analyses

Statistical analysis was done using GraphPad Prism Software (GraphPad). For *in vivo* xenograft data, one-way ANOVA and unpaired *t* tests with the two-tailed *P* value were used to evaluate for significant differences between the each drug concentration and control group. Statistical significance for this study was set at $P < 0.05$.

Results

Nurr1Expression and Structure-Dependent Transactivation by C-DIM

Figure 1A shows that Nurr1 protein is expressed in a panel of human bladder cancer cells including 253J B-V, 253J P, KU7, UM-UC3, UM-UC5, UM-UC6, UM-UC9, UM-UC10, UM-UC13, and UM-UC14 cells. Our group has identified C-DIMs containing a *p*-methoxy group (DIM-C-pPhOCH$_3$) or no substituents (DIM-C-Ph) as activators of NR4A-dependent transcription (17, 18). As indicated in Fig. 1B, DIM-C-pPhOCH$_3$, DIM-C-Ph, and DIM-C-Ph with *p*-chlorosubstituent (DIM-C-pPhCl) were analyzed for their transactivation in KU7 cells transfected with chimeric Nurr1-GAL4 and a GAL4 response elements linked to a luciferase reporter gene. The results showed that only DIM-C-pPhCl significantly induced transactivation with a maximal >25-fold increase observed for 10 μmol/L DIM-C-pPhCl, whereas <5-fold induction of luciferase activity was observed for Nur77-active DIM-C-pPhOCH$_3$ and DIM-C-Ph (Fig. 1B). Figure 1C shows that DIM-C-pPhCl activates luciferase activity in cells transfected with GAL4-Nurr1 but not GAL4-Nur77. We further investigated the activity of a series of DIM-C-pPhCl analogues for the activation of Nurr1, Nor1, Nur77, or RXR in KU7 cells transfected with GAL4-Nurr1/pGAL4, GAL4-Nor1/pGAL4, GAL4-Nur77/pGAL4, NuRE, PM-GAL4/pGAL4, or RXR-GAL4/pGAL4. As illustrated in Fig. 1D, DIM-C-pPhCl and its *N*-methyl and 2-methyl analogues all significantly activated GAL4-Nurr1; however, in parallel assays in KU7 cells, these compounds did not activate Nur77, Nor1, or RXR (a summary of these results is provided as Supplementary Data).[4] We selected DIM-C-pPhCl from among the three Nurr1-active compounds as a model for investigating downstream responses resulting from activation of Nurr1.

Nurr1-Active C-DIM Inhibits Bladder Cancer Cell Growth and Induces Apoptosis

In previous studies, we have shown that peroxisome proliferator-activated receptor γ-active C-DIMs such as DIM-C-pPhtBu and DIM-C-pPhC6H5 inhibit bladder cancer growth *in vitro* and *in vivo* (19). From our panel of cell lines, 253J B-V and KU7 cells are the most suitable for *in vivo* studies; hence, we focused on these cell line as models for investigating the activities of Nurr1-active C-DIM. Figure 2A shows that DIM-C-pPhCl inhibited KU7 and 253J B-V cell proliferation. Moreover, KU7 cells continuously exposed to increasing concentrations of DIM-C-pPhCl underwent dose-dependent apoptosis after 48 h as

[4]Supplementary material for this article is available at Molecular Cancer Therapeutics Online (http://mct.aacrjournals.org/).

measured by propidium iodide/fluorescence-activated cell sorting. DIM-C-pPhCl induced a modest increase in apoptosis at concentrations as low as 2.5 μmol/L with more significant apoptosis observed at concentrations of >5 μmol/L (Fig. 2B) and this included induction of TRAIL (Fig. 3A and B). Apoptosis induced by DIM-C-pPhCl after 48 h was accompanied by several markers of apoptosis, including PARP cleavage and dose-dependent activation of caspase-3, caspase-8, and caspase-9, along with TRAIL protein (Fig. 3A). In addition, DIM-C-pPhCl treatment induced these apoptosis-related proteins after 24 and 48 h, respectively (Fig. 3B). We further investigated the effect of pan-caspase inhibitor (z-VAD-fmk) on induction of PARP cleavage by DIM-C-pPhCl and showed that pretreatment of 253J B-V cells with pan-caspase inhibitor z-VAD-fmk abrogated DIM-C-pPhCl-induced cleavage of PARP (Fig. 3C). In addition, we also investigated the effects of DIM-C-PPhCl on induction of TRAIL mRNA levels in bladder cancer cells. Reverse transcription-PCR analysis showed that 5 μmol/L DIM-C-pPhCl induced TRAIL mRNA production (Fig. 3D) and this complemented the induction of TRAIL protein in bladder cancer cells (Fig. 3A and B).

DIM-C-pPhCl-Induced Apoptosis Is Dependent on Nurr1Expression

Because we hypothesized that DIM-C-pPhCl specifically activates Nurr1 (Fig. 1B–D) to induce apoptosis, the role of Nurr1 in mediating these proapoptotic responses was further investigated by RNA interference using Nurr1 siRNA. None of the bladder cancer cell lines tested lacked endogenous Nurr1 protein; hence, we took advantage of siRNA to Nurr1 to evaluate the effect of DIM-C-pPhCl on activation of this orphan receptor. In 253J B-V cells, transfection of Nurr1 siRNA significantly decreased Nurr1 expression (Fig. 4A and B) and decreased the ratio of cleaved PARP activity, TRAIL protein expression (Fig. 4A, C, and D), and apoptosis. siRNA of Nurr1 did not alter Nur77 protein levels (data not shown) and endogenous Nor1 protein was not found in bladder cancer lines tested. These results suggest that Nurr1 protein is a key mediator of DIM-C-pPhCl-induced apoptosis.

Nurr1-Active C-DIM Results in a Reduction of Tumor Growth in Orthotopic Bladder Cancer Model in Nude Mice

To determine the effect of the Nurr1-active C-DIM on *in vivo* growth of bladder tumors, 253J B-V bladder xenograft tumors harboring lentivirus-mediated luciferase gene were established by transplanting the tumor cells orthotopically in the bladder wall of nude mice. DIM-C-pPhCl significantly inhibited the growth of orthotopic 253J B-V xenografts at doses of 12.5 and 25 mg/kg (Fig. 5A). After treatment for 4 weeks, the mice were sacrificed and tumor volumes were measured. When compared with the untreated group, mice treated with 12.5 and 25 mg/kg DIM-C-pPhCl showed 44% and 59% inhibition of tumor growth, respectively (Fig. 5B). Furthermore, mice treated with C-DIM had increased survival, which was statistically significant by the log-rank test (Fig. 5C; $P < 0.001$).

DIM-C-pPhCl Inhibits Proliferation and Induces DNA Fragmentation in Human BladderTumor Xenograft

H&E staining patterns showed large pockets of dead tissue in the DIM-C-pPhCl-treated orthotopic 253J B-V xenografts tumors (Fig. 6A, *arrowhead*). To assess the degree of inhibition of cell proliferation, we performed immunohistochemical staining for PCNA. The tumor sections from mice treated with 12.5 and 25 mg/kg DIM-C-pPhCl showed significant

23% and 47% decrease in the percentage of PCNA-positive cells (Fig. 6B). Tumor sections were also stained for TUNEL to ascertain the degree of DNA fragmentation (apoptosis). TUNEL staining in tumor sections from mice treated with 12.5 and 25 mg/kg Nurr1-active C-DIM showed a 52% and 82% increase ($P < 0.01$) in TUNEL-positive nuclei compared with controls (Fig. 6C).

Discussion

Recently, the nuclear receptor family of transcription factors has been found to be clinically relevant in different scenarios. Nerve growth factor I-B (NGFI-B) is part of a subfamily of orphan nuclear receptors that were initially identified after treatment of PC12 pheochromacytoma cells with NGF. Members of this subfamily include Nur77 (NGFI-Bα, TR_3), Nurr1 (NGFI-Bβ), and Nor1 (NGFI-Bγ). The physiologic roles for NGFI-B proteins are not fully understood; however, gene targeting knockout experiments show several important functions of these proteins, which correlate, in part, with other *in vitro* and *in vivo* studies. Early studies showed the robust expression of Nur77 during T-cell receptor-mediated apoptosis, suggesting a possible role for Nur77 in negative selection of thymocytes (20). Previous studies (21) have shown that stimulation of Nur77 with various agents leads to up-regulation of apoptosis-related proteins and these observations were confirmed and extended by our studies on a series of synthetic C-DIM analogues (18–22). Although Nurr1 is structurally related to ligand-activated nuclear receptors, Nurr1 is functionally atypical due to its inability to bind a cognate ligand and to activate transcription. Nurr1 knockout mice have severe impairments in midbrain neuronal development and dopamine expression, and these animals die soon after birth; but at this time, not much more is known about basal Nurr1 function or activation of Nurr1 (23). It has been suggested that Nurr1 exerts its functions through activation and subsequent induction of complex pathways of cell survival and apoptosis (23).

We present the first demonstration of a novel compound that activates Nurr1. In addition, our results also reveal a potential application of Nurr1-active C-DIM as a tumor-suppressing agent for bladder cancer. Initial studies confirmed that Nurr1 protein is highly expressed in bladder cancer cell lines (Fig. 1A) and our preliminary studies indicate that Nurr1 is overexpressed in bladder tumors obtained from patients sample (data not shown). DIM-C-pPhCl activated Nurr1/GAL4 but not Nurr77/GAL4 in bladder cancer cells (Fig. 1C) and also inhibited bladder cancer cell proliferation (Fig. 2A). The ability of activated Nurr1 to inhibit the growth of bladder cancer cells was due in part of induction of apoptosis in various bladder cancer cells (Fig. 3A and B). In the present study, a significant increase in cells in the sub-G_1 phase, accounting for 25.0% of the total cell population, was detected after exposure of KU7 cells to 5 μmol/L DIM-C-pPhCl (Fig. 2B). Assessment of the activation and cleavage of apoptosis-related proteins by Western blot analysis further confirmed that DIM-C-pPhCl induced KU7 and 253J B-V bladder cancer cells to undergo apoptosis in a dose- and time-dependent fashion, respectively (Fig. 3). Treatment of KU7 and 253J B-V bladder cancer cells with DIM-C-pPhCl resulted in PARP cleavage along with induction of the death receptor ligand TRAIL. Moreover, the involvement of pro-caspase-3, pro-caspase-8, and pro-caspase-9 cleavage to active forms was also observed in 253J B-V and KU7 cells treated with DIM-C-pPhCl. Thus, induction of apoptosis in bladder cancer cells

by the Nurr1-active C-DIM was confirmed by several methods. The role of Nurr1 in inducing the proapoptotic responses was further solidified by RNA interference using transfected iNurr1, which significantly decreased Nurr1 expression (Fig. 4A and B). Importantly, DIM-C-pPhCl-induced TRAIL protein expression and PARP cleavage were also significantly decreased in cells transfected with iNurr1 (Fig. 4A, C, and D). Previous studies showed that Nur77-active DIM-C-pPhOCH$_3$ and DIM-C-Ph induce TRAIL expression in colon and pancreatic cancer cells (22) and we have also observed similar results in bladder cancer cells. Induction of TRAIL and PARP cleavage by DIM-C-pPh-OCH$_3$ in colon cancer cells was inhibited after cotransfection with a siRNA for Nur77 (22) and this paralleled the Nurr1-dependent induction of TRAIL in bladder cancer cells (Figs. 3 and 4) observed in this study. Thus, two structurally related C-DIM compounds, which differ only in a single *p*-chloro versus methoxy substituent, resulted in selective activation of Nurr1 and Nur77 to induce expression of the same gene product, that is, TRAIL. The structure-dependent selectivity in activating Nurr1 by DIM-C-pPhCl (Fig. 1B and C), Nur77, by DIM-C-pPhOCH$_3$ (22) and the failure to activate Nor1 and RXR (Supplementary Data)[4] does not necessarily mean that these compounds are ligands for Nurr1 or Nur77 and current studies are focused the molecular mechanisms of receptor activation. The induction of TRAIL by DIM-C-pPhCl (Figs. 3 and 4) and the Nur77-active DIM-C-pPh-OCH$_3$ is not unexpected because both nuclear receptors interact with common response elements in target gene promoters (23). These results confirm that proapoptotic responses induced by DIM-C-pPhCl were Nurr1 dependent; however, this does not exclude a contribution of Nurr1-independent proapoptotic response induced by this compound (24, 25). Nurr1 may also play a role in angiogenesis and this is currently being investigated in our laboratories.

We also investigated the *in vivo* antitumorigenic activity of DIM-C-pPhCl by implanting the highly tumorigenic 253J B-V cells into the bladders of athymic nude mice. DIM-C-pPhCl inhibited bladder tumor growth and decreased PCNA and increased TUNEL staining in tumors, which was comparable with similar responses, observed in bladder cancer cells (Fig. 6B). This is the first report of the antitumorigenic activity of a compound that acts through activation of Nurr1 in an *in vivo* model of bladder cancer.

In conclusion, we present data that establish a novel Nurr1-active C-DIM as a potent and specific stimulator of the Nurr1-apoptosis axis in bladder cancer cells and tumors. The link between heightened activity of this orphan receptor and an antitumor response may involve myriad and divergent events. However, by identifying a compound that activates a pivotal proapoptotic Nurr1-dependent signaling pathway with known antitumor potential, we hope to further our understanding of both the mechanism of action of this promising new therapeutic agent and the role of Nurr1 in human bladder cancers.

Acknowledgments

Grant support: National Cancer Institute Bladder Cancer Specialized Program of Research Excellence grant CA 91846 and NIH grants CA 16672 and CA 124998.

References

1. Jemal A, Siegel R, Ward E, et al. Cancer statistics, 2008. CA Cancer J Clin. 2008; 58:71–96. [PubMed: 18287387]
2. Dinney CP, McConkey DJ, Millikan RE, et al. Focus on bladder cancer. Cancer Cell. 2004; 6:111–6. [PubMed: 15324694]
3. Bajorin DF, Dodd PM, Mazumdar M, et al. Long-term survival in metastatic transitional-cell carcinoma and prognostic factors predicting outcome of therapy. J Clin Oncol. 1999; 17:3173–81. [PubMed: 10506615]
4. Steinmetz AC, Renaud JP, Moras D. Binding of ligands and activation of transcription by nuclear receptors. Annu Rev Biophys Biomol Struct. 2001; 30:329–59. [PubMed: 11340063]
5. Wansa KD, Harris JM, Muscat GE, et al. The activation function-1 domain of Nur77/NR4A1 mediates trans-activation, cell specificity, and coactivator recruitment. J Biol Chem. 2002; 277:33001–11. [PubMed: 12082103]
6. Hazel TG, Nathans D, Lau LF. A gene inducible by serum growth factors encodes a member of the steroid and thyroid hormone receptor superfamily. Proc Natl Acad Sci U S A. 1988; 85:8444–8. [PubMed: 3186734]
7. Pei L, Waki H, Vaitheesvaran B, et al. NR4A orphan nuclear receptors are transcriptional regulators of hepatic glucose metabolism. Nat Med. 2006; 12:1048–55. [PubMed: 16906154]
8. Le WD, Xu P, Jankovic J, et al. Mutations in NR4A2 associated with familial Parkinson disease. Nat Genet. 2003; 33:85–9. [PubMed: 12496759]
9. Chen YH, Tsai MT, Shaw CK, et al. Mutation analysis of the human NR4A2 gene, an essential gene for midbrain dopaminergic neurogenesis, in schizophrenic patients. Am J Med Genet. 2001; 105:753–7. [PubMed: 11803525]
10. Buervenich S, Carmine A, Arvidsson M, et al. NURR1 mutations in cases of schizophrenia and manic-depressive disorder. Am J Med Genet. 2000; 96:808–13. [PubMed: 11121187]
11. Newman SJ, Bond B, Crook B, Darker, et al. Neuron-specific localisation of the TR3 death receptor in Alzheimer's disease. Brain Res. 2000; 857:131–40. [PubMed: 10700560]
12. Glass CK, Rosenfeld MG. The coregulator exchange in transcriptional functions of nuclear receptors. Genes Dev. 2000; 14:121–41. [PubMed: 10652267]
13. Jacobsen KX, MacDonald H, Lemonde S, et al. A Nurr1 point mutant, implicated in Parkinson's disease, uncouples ERK1/2-dependent regulation of tyrosine hydroxylase transcription. Neurobiol Dis. 2008; 29:117–22. [PubMed: 17890097]
14. Wu Q, Liu S, Ye XF, et al. Dual roles of Nur77 in selective regulation of apoptosis and cell cycle by TPA and ATRA in gastric cancer cells. Carcinogenesis. 2002; 23:1583–92. [PubMed: 12376465]
15. Dinney CP, Fishbeck R, Singh RK, et al. Isolation and characterization of metastatic variants from human transitional cell carcinoma passaged by orthotopic implantation in athymic nude mice. J Urol. 1995; 154:1532–8. [PubMed: 7658585]
16. Qin C, Morrow D, Stewart J, et al. A new class of peroxisome proliferator-activated receptor γ (PPARγ) agonists that inhibit growth of breast cancer cells: 1,1-bis(3′-indolyl)-1-(*p*-substituted phenyl)methanes. Mol Cancer Ther. 2004; 3:247–60. [PubMed: 15026545]
17. Hadaschik BA, Black PC, Sea JC, et al. A validated mouse model for orthotopic bladder cancer using transurethral tumour inoculation and bioluminescence imaging. BJU Int. 2007; 100:1377–84. [PubMed: 17850390]
18. Chintharlapalli S, Burghardt R, Papineni S, et al. Activation of Nur77 by selected 1,1-bis(3′-indolyl)-1-(*p*-substituted phenyl)methanes induces apoptosis through nuclear pathways. J Biol Chem. 2005; 280:24903–14. [PubMed: 15871945]
19. Kassouf W, Chintharlapalli S, Abdelrahim M, et al. Inhibition of bladder tumor growth by 1,1-bis(3′-indolyl)-1-(*p*-substituted phenyl)methanes: a new class of peroxisome proliferator-activated receptor γ agonists. Cancer Res. 2006; 66:412–8. [PubMed: 16397256]
20. Calnan BJ, Szychowski S, Chan FK, et al. A role for the orphan steroid receptor Nur77 in apoptosis accompanying antigen-induced negative selection. Immunity. 1995; 3:273–82. [PubMed: 7552993]

21. Lin B, Kolluri SK, Lin F, et al. Conversion of Bcl-2 from protector to killer by interaction with nuclear orphan receptor Nur77/TR3. Cell. 2004; 116:527–40. [PubMed: 14980220]
22. Cho SD, Yoon K, Chintharlapalli S, et al. Nur77 agonists induce proapoptotic genes and responses in colon cancer cells through nuclear receptor-dependent and nuclear receptor-independent pathways. Cancer Res. 2007; 67:674–83. [PubMed: 17234778]
23. Sacchetti P, Carpentier R, Segard P, et al. Multiple signaling pathways regulate the transcriptional activity of the orphan nuclear receptor NURR1. Nucleic Acids Res. 2006; 34:5515–27. [PubMed: 17020917]
24. Abdelrahim M, Newman K, Vanderlaag K, et al. 3,3′-Diindolylmethane (DIM) and its derivatives induce apoptosis in pancreatic cancer cells through endoplasmic reticulum stress-dependent upregulation of DR5. Carcinogenesis. 2006; 27:717–28. [PubMed: 16332727]
25. Cho SD, Lei P, Abdelrahim M, et al. 1,1-Bis(3′-indolyl)-1-(*p*-methoxyphenyl)methane activates Nur77-independent proapoptotic responses in colon cancer cells. Mol Carcinog. 2008; 47:252–63. [PubMed: 17957723]

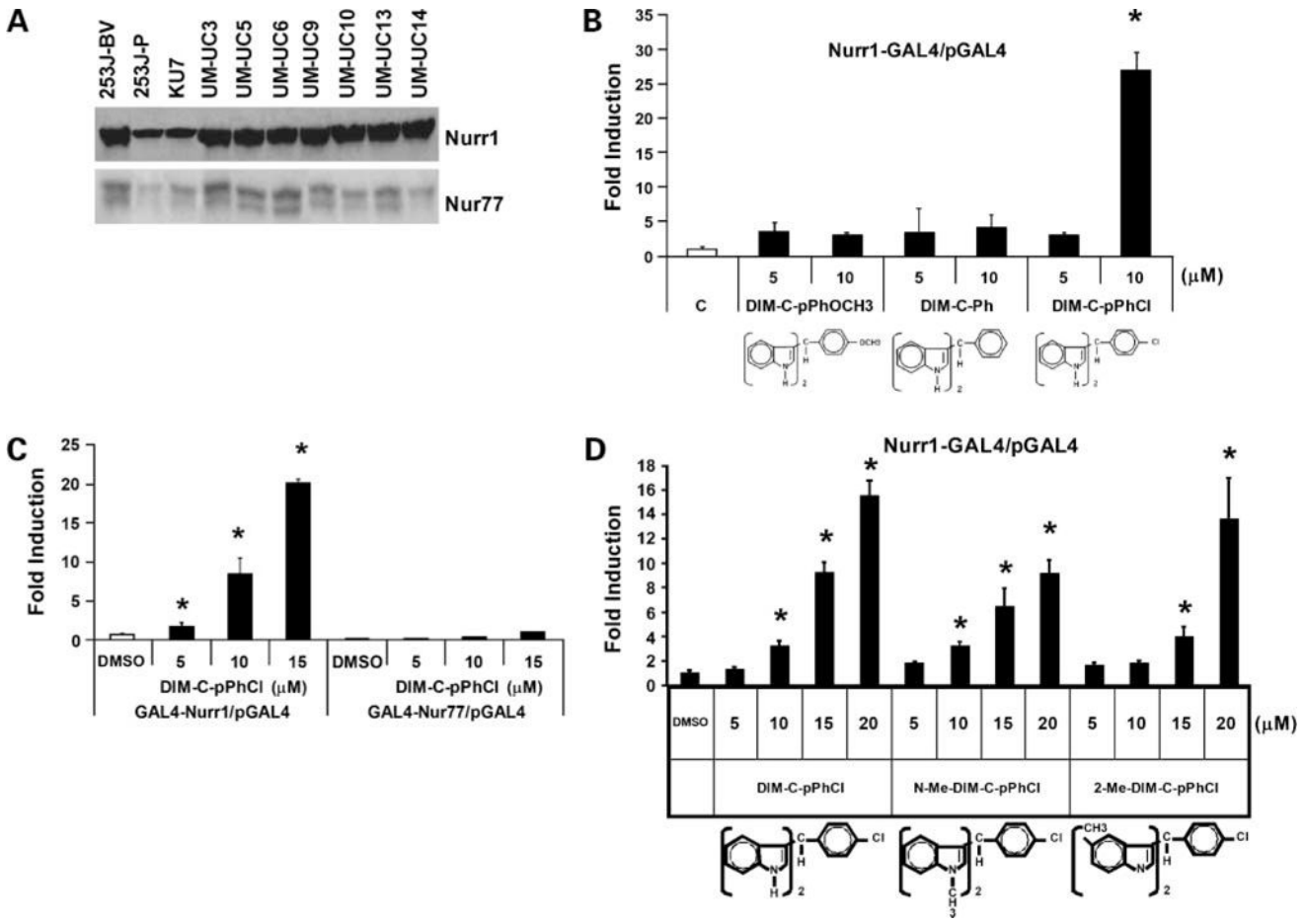

Figure 1.

Expression of Nurr1 and Nur77 protein in urothelial carcinoma cells and structure-dependent Nurr1 activation by C-DIM. **A**, Nurr1 and Nur77 expression in bladder cancer cells. Whole-cell lysates from 253J B-V, 253J P, KU7, UM-UC3, UM-UC5, UM-UC6, UM-UC9, UM-UC10, UM-UC13, and UM-UC14 cells were analyzed by Western blot analysis as described in Materials and Methods. **B** to **D**, activation of GAL4-Nurr1/pGAL4, GAL4-Nor1/pGAL4, GAL4-Nur77/pGAL4, NuRE, PM-GAL4/pGAL4, or RXR-GAL4/pGAL4 by C-DIM compounds. KU7 bladder cancer cells were transfected with GAL4-Nurr1/pGAL4, GAL4-Nor1/pGAL4, GAL4-Nur77/pGAL4, NuRE, PM-GAL4/pGAL4, or RXR-GAL4/pGAL4 and treated with DMSO or different concentrations of the C-DIMs and luciferase. *Columns*, mean of at least three replicate experiments for each treatment group; *bars*, SE. *, $P < 0.05$.

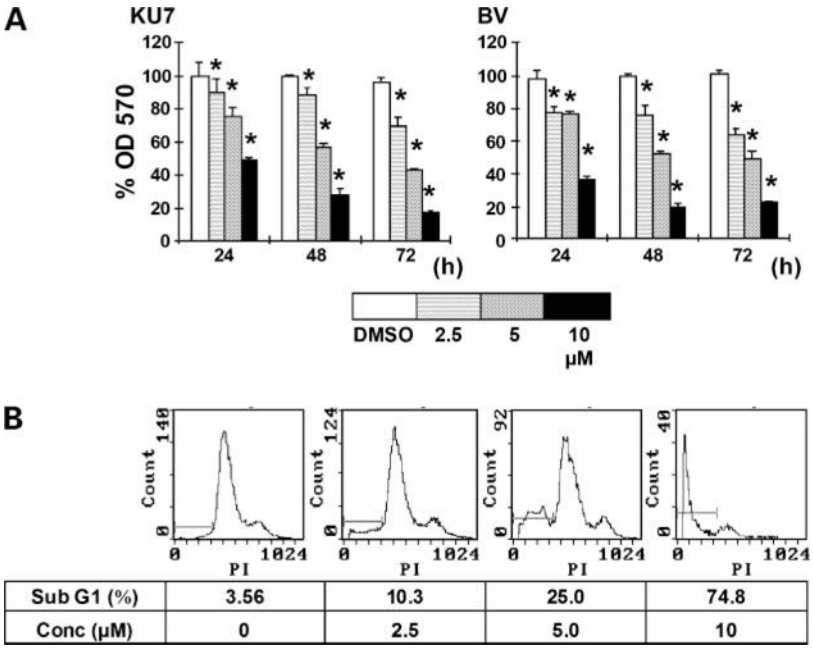

Sub G1 (%)	3.56	10.3	25.0	74.8
Conc (μM)	0	2.5	5.0	10

Figure 2.

Nurr1-active C-DIM-induced growth inhibition of urothelial carcinoma cells. **A**, time- and concentration-dependent effects of DIM-C-pPhCl on KU7 and 253J B-V cell proliferation. Cell were treated with DMSO or 2.5, 5, or 10 μmol/L DIM-C-pPhCl for 24, 48, and 72 h, and the percentage proliferation was determined where the number of cells in the solvent-treated (DMSO) group was set at 100%. *Columns*, mean of three replicate experiments for each concentration; *bars*, SE. *, $P < 0.05$. **B**, concentration-dependent induction of apoptosis by DIM-C-pPhCl on KU7 cells. KU7 cells were treated with the indicated concentrations of DIM-C-pPhCl for 48 h. Cells were then harvested, and DNA fragmentation characteristic of apoptosis was measured by propidium iodide staining and fluorescence-activated cell sorting analysis.

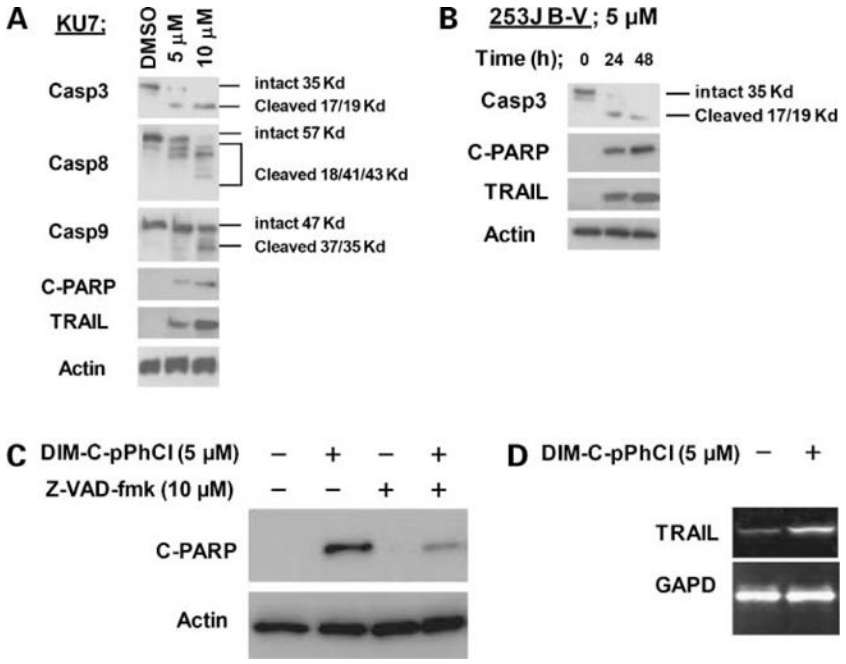

Figure 3.

Effects of DIM-C-pPhCl on apoptosis. **A**, dose-dependent induction of apoptosis in KU7 cells by DIM-C-pPhCl. KU7 cells were treated with different concentrations of DIM-C-pPhCl for 48 h, and whole-cell lysates were analyzed by Western blot analysis. **B**, time-dependent induction of apoptosis by DIM-C-pPhCl in 253J B-V cells. 253J B-V cells were treated with 5 μmol/L C-DIM-pPhCl for 24 and 48 h, and whole-cell lysates were analyzed by Western blot analysis. **C**, effects of z-VAD-fmk in PARP cleavage. 253J B-V cells were treated with DIM-C-pPhCl alone or in combination with 10 μmol/L pan-caspase inhibitor z-VAD-fmk, which was administrated 1 h before the addition of 5 μmol/L DIM-C-pPhCl. After 48 h, whole-cell lysates were analyzed for cleaved PARP and TRAIL induction by Western blot analysis as described in Materials and Methods. **D**, induction of TRAIL mRNA by DIM-C-pPhCl in T24 cells. cDNAs were generated from 1 μg total RNAs from bladder cancer cells with or without 5 μmol/L DIM-C-pPhCl. Reverse transcriptase reaction was carried as described in Materials and Methods.

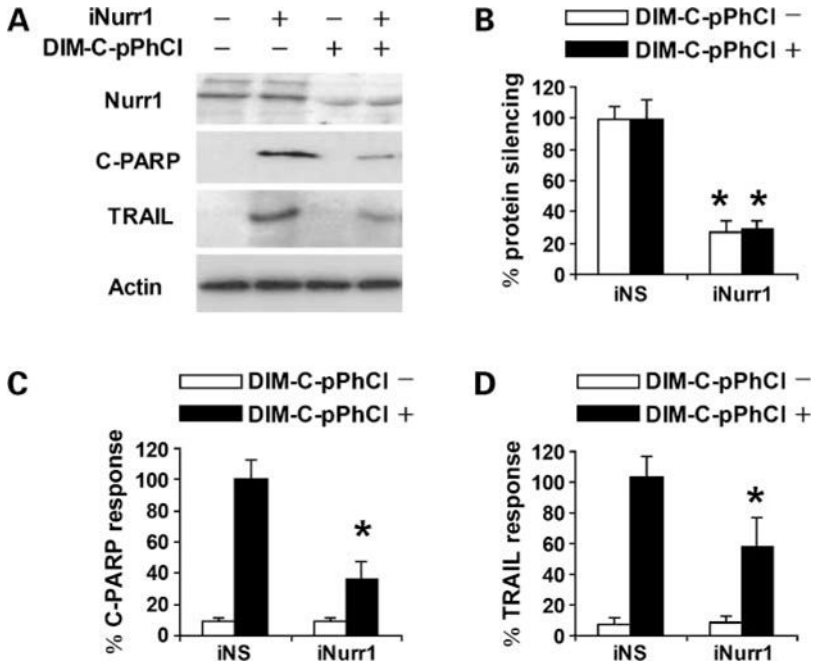

Figure 4.

Nurr1-dependent induction of TRAIL and cleaved PARP in 253J B-V cells. Cells were transfected with nonspecific control (*iNS*) or iNurr1 and treated with DMSO or 10 μmol/L DIM-C-pPhCl, and whole-cell lysates were analyzed by Western blot analysis for Nurr1, PARP cleavage, TRAIL, and actin (loading control) proteins (**A**). *Columns*, mean of three replicate experiments for each treatment group; *bars*, SE. Protein levels were normalized to actin. Significant ($P < 0.05$) inhibition of Nurr1 expression (**B**), decreased expression induction of PARP cleavage (**C**), and TRAIL (**D**) by iNurr1 are quantitated and 100% protein expression was assigned to levels in cells treated with DIM-C-pPhCl and transfected with nonspecific control. Each experiment was reproduced three times independently.

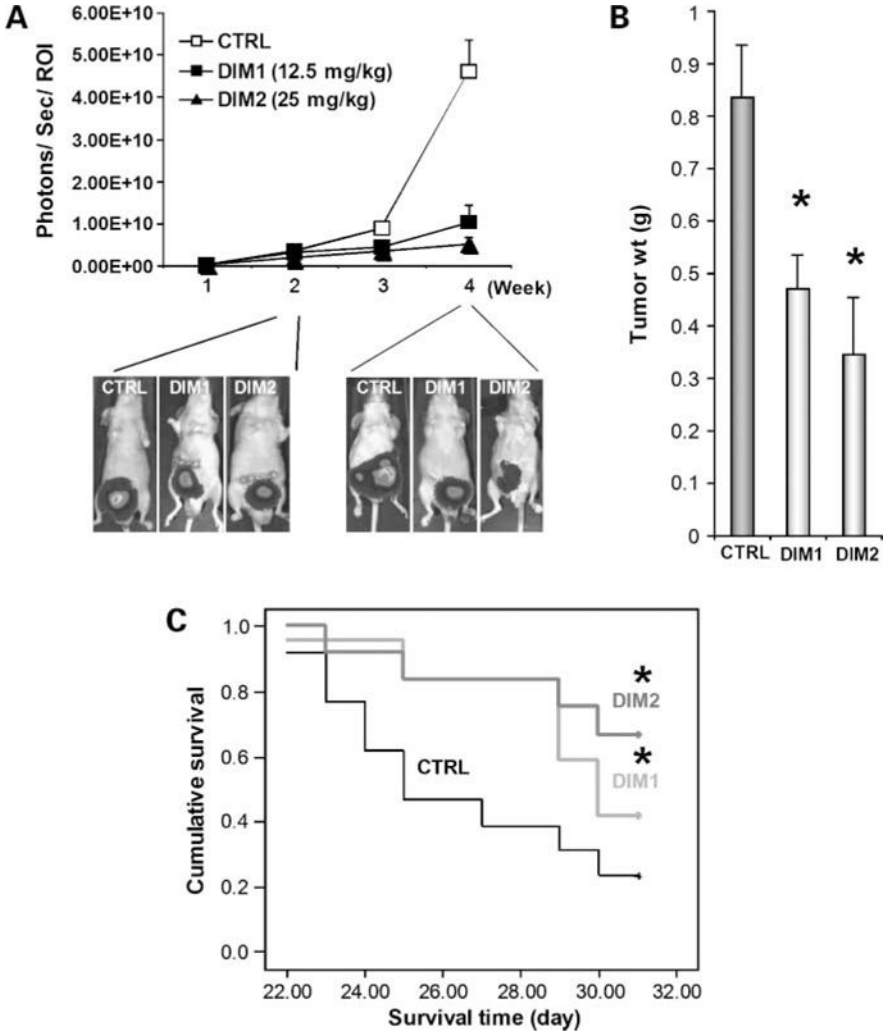

Figure 5. In vivo

anticarcinogenic activity of DIM-C-pPhCl. **A**, effects of DIM-C-pPhCl on primary bladder tumors. Three different treatment groups consist of DMSO control (*CTRL; n* = 14), 12.5 mg/kg/d DIM-C-pPhCl (*DIM1; n* = 13), and 25 mg/kg/d DIM-C-pPhCl (*DIM2; n* = 13). Each group was treated thrice a week right after randomization. 253J B-V cells (2×10^5) were implanted into bladder wall of male nude mice. Mice were injected with luciferin i.p. and were imaged on the charge-coupled device camera 10 min after injection. Bioluminescent imaging images were collected for 1 or 10 s for each group. Different image acquisition times were needed to avoid saturating the charge-coupled device camera. Bioluminescence is presented as a pseudocolor scale: *red*, highest photon flux; *blue*, lowest photon flux. Bioluminescence from primary tumors was quantified by region of interest analysis of images obtained on the indicated time points (*X axis*) after cell implantation. Background bioluminescence was subtracted from each tumor region of interest value. Mean ± SE photon flux in each group. *Bottom*, representative bioluminescent imaging images of primary 253J B-V bladder tumors 2 and 4 wk after initial treatment. **B**, tumor size measurements. Actual tumor sizes were measured 4 wk after implantation of cancer cells. Mean ± SE tumor volume. *, $P < 0.05$. **C**, effects of DIM-C-pPhCl on human bladder

xenograft mice survival. Kaplan-Maier plots were generated, and survival time of animals was analyzed for significance by log-rank survival analysis. *, $P < 0.05$.

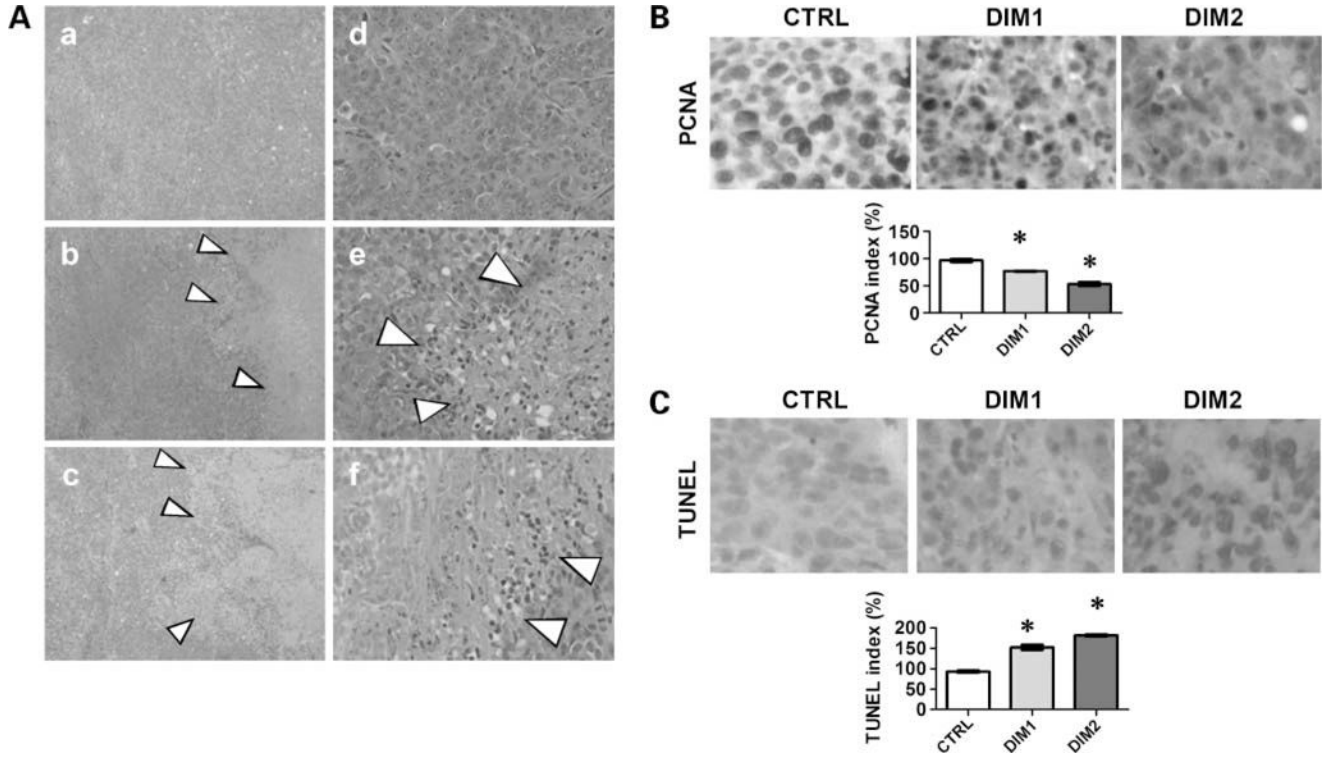

Figure 6.

Histopathologic changes of mice tumor after DIM-C-pPhCl treatment. **A**, H&E staining of tumor from DMSO control [original magnification, ×40 (*a*) and ×200 (*d*)], 12.5 mg/kg/d DIM-C-pPhCl [original magnification, ×40 (*b*) and ×200 (*e*)], and 25 mg/kg/d DIM-C-pPhCl [original magnification, ×40 (*c*) and ×200 (*f*)]. Grouping was determined as described in Materials and Methods. **B**, PCNA staining of DMSO control (original magnification, ×200), 12.5 mg/kg/d DIM-C-pPhCl (original magnification, ×200), and 25 mg/kg/d DIM-C-pPhCl (original magnification, ×200). Grouping were determined as described in Materials and Methods. Proliferation was determined using PCNA index. *CTRL*, control; *DIM1*, 12.5 mg/kg/d DIM-C-pPhCl; *DIM2*, 25 mg/kg/d DIM-C-pPhCl. To calculate PCNA index, the tissue was photographed using Optotronics Tec 470 camera linked to a computer and digital printer. The intensity of the immunostaining was quantified in multiple points in five different areas of each sample by an image analyzer using Optimas image analysis software (Media Cybernetics) to obtain an average measurement. The density of proliferative cells was expressed as an average of the five highest densities identified within a single ×200 field. *, $P < 0.05$. **C**, TUNEL staining of DMSO control (original magnification, ×200), 12.5 mg/kg/d DIM-C-pPhCl (original magnification, ×200), and 25 mg/kg/d DIM-C-pPhCl (original magnification, ×200). Grouping were determined as described in Materials and Methods. Apoptosis of bladder tumors was quantified for TUNEL expression. *, $P < 0.05$.